Japanese Journal of Applied Physics
Vol. 45, No. 4A, 2006, pp. 2875–2880

©2006 The Japan Society of Applied Physics

Effective Light Absorptive Layer Using Mezo-Porous Silicon by Electrochemical Etching

Jae-Hong KWON, Soo-Hong LEE[1] and Byeong-Kwon JU*

School of Electrical Engineering, College of Engineering Korea University, Seoul 136-701, Korea
[1]*Strategic Energy Research Institute, Sejong University, Seoul 143-747, Korea*

(Received July 16, 2005; accepted December 26, 2005; published online April 7, 2006)

Porous silicon (PS), an excellent light diffuser, can be used as an antireflective layer that does not need to be coated with other antireflection coating (ARC) materials. PS layers were obtained by electrochemical etching (ECE) anodization of silicon wafers in hydrofluoric acid/ethanol/deionized (DI) water solution (HF/EtOH/H_2O). This technique selectively removes Si atoms from the sample surface, forming a PS layer with adjustable optical, electrical, and mechanical properties. A PS layer with optimal antireflection characteristics was obtained for a charge density (Q) of $5.2\,C/cm^2$. The weighted reflectance was reduced from 24 to 4% in the wavelength range from 400 to 1000 nm. The weighted reflectance with optimized PS layers is much less than that with a commercial SiN_X ARC on a potassium hydroxide (KOH) pretextured multicrystalline silicon (mc-Si) surface. Therefore, it can be successfully used as an alternative way for the preparation of a PS antireflective layer for a silicon solar cell. [DOI: 10.1143/JJAP.45.2875]

KEYWORDS: electrochemical etching, porous silicon, antireflective layer, solar cell

1. Introduction

Light trapping is an important method of increasing the efficiency of crystalline silicon solar cells. Several other techniques, such as the surface antireflection coating (ARC)[1] and texturization,[2] have been widely used for the same purpose. Commercial multicrystalline silicon (mc-Si) solar cells have, in general, silicon nitride (SiN_X) films that not only act as an ARC with a suitable refractive index, but also improve the performance of photovoltaic devices by defect, surface and bulk passivation. However, the formation of the SiN_X films by plasma enhanced chemical vapor deposition (PECVD)[3] is a costly process. On the other hand, recently, simple and cost-down techniques that use chemical solutions have been developed to solve the cost problem. For example, alkaline enchants composing sodium hydroxide (NaOH) or KOH with isopropyl alcohol (IPA) as an organic agent are widely used to texture monocrystalline silicon (mono-Si).[4] However, this method is not efficient for mc-Si because only a certain fraction of the grains have a (100) crystallographic orientation. Acidic etching using HF and nitric acid (HNO_3), which act as strong oxidizing agents, has been used to texture the surface of mc-Si.[5] However, with this technique, it is also difficult to control the uniformity of the Si wafer surface and layer thickness, and other new approaches have also been studied.[6,7] In this paper, we first present a summary of our experimental results regarding the formation of single porous silicon (PS) antireflective layers. PS developed on a crystalline Si wafer surface drastically reduces optical losses by acting as an ARC layer.[8,9] We studied the PS etching of mc-Si for photovoltaic applications. This process has several advantages, such as the production of reflectance lower than that of the deposited single ARC layer, no vacuum processes or toxic gasses, PS formation in $<35\,s$ with a good repeatability, simplicity and a low cost. An antireflective layer can be optimized by tailoring the porosity (or refractive index) of the PS layer for a given cell structure. Through this optimization, the surface geometry can be optimized. Since PS texturing does not depend on the crystallographic orientation, mc-Si can be uniformly textured on the entire wafer when the mc-Si surface is supplied with a high current density. Furthermore, when phosphosilicate glass (PSG) remaining after dopant diffusion is simultaneously removed, a substrate cleaning process can be eliminated. The PS etching behavior studied in this work can be used to determine the thickness and porosity profiles of electrochemically etched PS layers on the basis of technological parameters[10] and can be used to set the etching conditions providing the lowest surface reflectance. We present several promising results: our technique provides a weighted reflectance that is 4% lower than those of other techniques. Moreover, we performed a PS solar cell process with PS formation after selective emitter formation.[11]

2. Materials

Uhlir discovered PS in 1956 while using an HF-containing electrolyte to carry out electropolishing experiments on a Si wafer. He found that the Si wafer dissolved partially as the current was increased over a certain threshold.[12] PS was formed by the electrochemical dissolution of the Si wafer in aqueous or ethanoic HF solutions. The main requirements for PS formation are as follows: The Si wafer must be anodically biased, that is, forward biasing for p-type doped Si, reverse biasing for n-type doped Si, and light requirement for n-type doped and semi-insulating p-type doped Si.[13]

In the case of current flow through the Si wafer, the reaction was accomplished by making the silicon wafer the anode, and thus, a positive charge can be delivered to the wafer surface. This is often referred to as anodization. Depending on the current density, either electropolishing or porous etching was achieved. Using a low current density caused a limited hole (h^+) injection at the surface of the Si anode, and therefore, only localized pits were formed, resulting in a PS surface. When a sufficiently high current density was achieved, the surface was saturated with holes (h^+) and polishing occurred.[14]

Ethanoic solution infiltrates the pore, but purely aqueous HF solution does not, which is very important for the lateral homogeneity and uniformity of the PS layer in depth. In addition, during the reaction, hydrogen (H_2) is released. Bubbles form and stick on the Si surface in pure aqueous solutions, but they can be removed using EtOH (or other surfactants). The porosity and pore size are increased using reduced HF and elevated EtOH. The thickness increases

*Corresponding author. E-mail address: bkju@korea.ac.kr

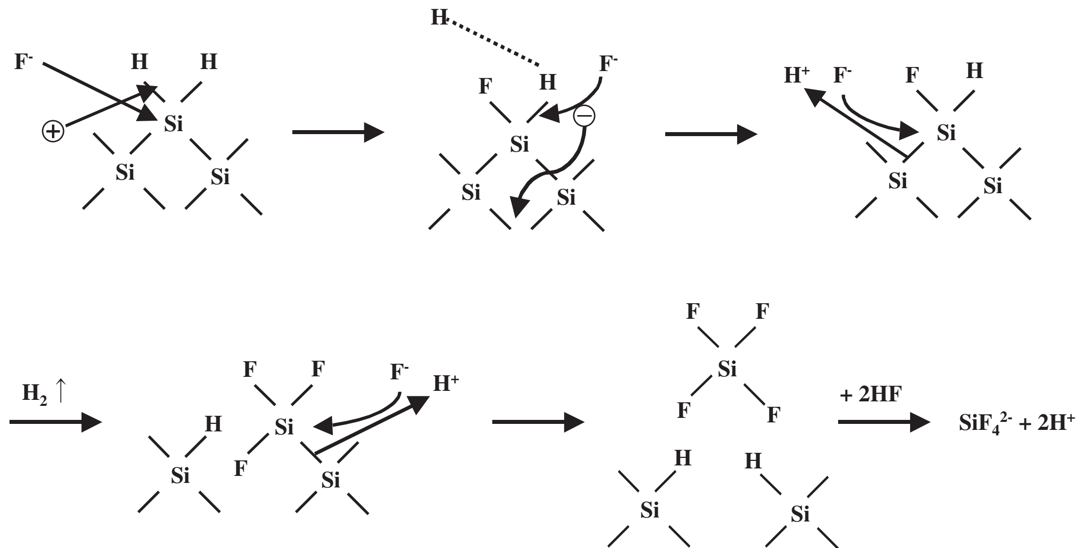

Fig. 1. Schematic representation of pore formation chemistry based on mechanism proposed by Allongue *et al.*[15)]

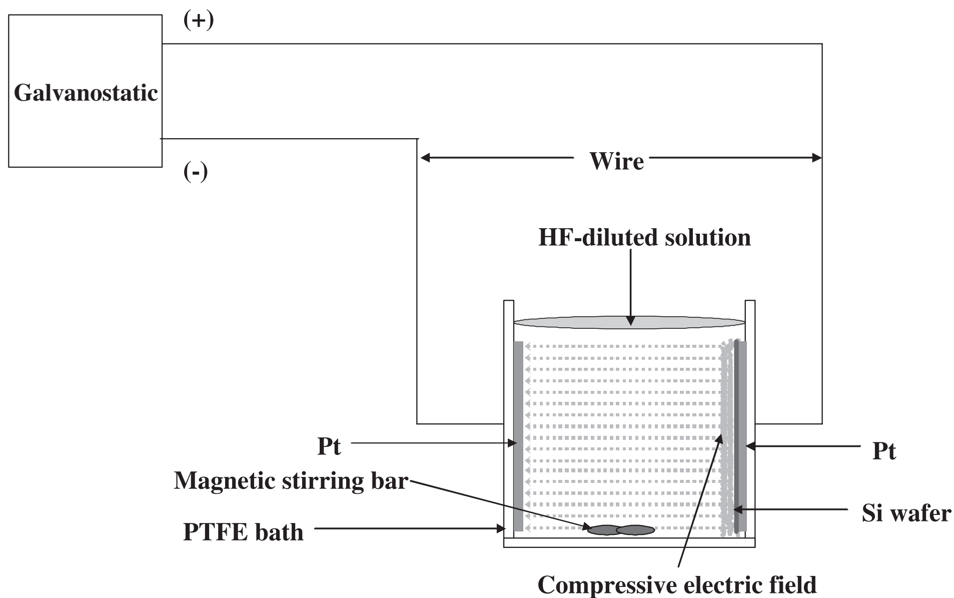

Fig. 2. Schematic drawing of anodic ECE bath used for PS preparation.

with HF concentration but decreases with EtOH concentration. A long etching ECE time leads to the formation of a thick layer; however, this layer becomes anisotropic with depth due to the chemical reaction of the electrolytes HF and EtOH with solution compositions.

Figure 1 shows the schematic representation of the chemistry of pore formation based on the mechanism proposed by Allongue *et al.*[15)] For PS formation, it is essential that the Si surface saturated by H_2 is virtually inert against further attack of fluoride ions (F^-) as long as no electronic holes (h^+) are available at the Si electrode, because the electronegativity of H is about the same as that of Si and as long as the induced polarization is low. If a hole (h^+) reaches the surface, nucleophilic attack on Si–H bonds by fluoride ions can occur and a Si–F bond can be established (Step 1 in Fig. 1.). Due to the polarizing influence of the bonded F, another F^- ion can attack and bond during the generation of a H_2 molecule and the injection of one electron into another electron and then into the electrode (Step 2). Due to the polarization induced by the Si–F groups, the electron density of the Si–Si backbonds decreases, and these weakened bonds are attacked by HF or H_2O (Steps 4 and 5) in a way that the Si surface atoms remain bonded to H_2 (Step 5). If a Si atom is removed from an atomically flat surface by this reaction, an atomic size dip remains. This change in surface geometry changes the electric field distribution in such a way that holes (h^+) transfer from this location preferentially. Therefore, surface inhomogeneities are amplified.

3. Experimental

The starting material was a boron-doped *p*-type mc-Si wafer (Eurosolar) with a resistivity range from 0.5 to 2 Ω cm and a sample area of $2 \times 2\,cm^2$. First, for the mc-Si surface, the etching of sawing damage was performed in a KOH solution. Next, the wafer was cleaned by RCAs I and II in

the boiled solutions ($H_2O : H_2O_2 : NH_3OH = 7 : 1 : 1$) and ($H_2O : H_2O_2 : HCl = 7 : 1 : 1$), respectively, and dipped into (5%) HF for several seconds to remove any native surface oxide and any residual contamination from the solutions. Electrochemical anodization was performed using a mixed solution (i.e., 3 : 1 volume ratio mixture of 49% HF solution and absolute EtOH). PS formation was achieved by ECE with a mutichannel potentiostat/galvanostat (WonA-Tech, WonATech WMPG 1000). Anodization current density (125–270 mA/cm^2) and duration (10–35 s) were controlled by computer-driven potential-stabilized electrolyte bath. The bath contained polytetrafuorethylene (PTFE), and a platinum (Pt) electrode was used as a cathode. A counterelectrode was used as a Si wafer/Pt. The principle of the equipment is schematically shown in Fig. 2. The bath was agitated using a magnetic stirring bar to prevent H_2 bubbling over the etching surface, and thus, a more uniform PS structure was fabricated. After PS formation, samples were rinsed with DI water and dried immediately after anodic ECE to prevent the PS film from flaking and deterioration (i.e., the samples are dried in N_2 gas and stored). The weighted reflectance measurements were carried out using reflectance (Newport, Oriel 70111) in the 300–1000 nm wavelength range. We compared the reflectance characteristics of the optimized SiN_X layer deposited by plasma-enhanced chemical vapor deposition (PECVD; Centrotherm Photovoltaics, E-2000) with those of the PS layer. The surface morphology of the electrochemically etched PS layer was observed using a field emission scanning electron microscope (FE-SEM; Hitachi, Hitachi S-4300 Unit). The anodic ECE of Si, from which we obtained the thickness and porosity of the PS layer, was performed using a spectroscopic ellipsometer (SE; Jobin Yvon, UNISEL spectroscopic phase modulated ellipsometer).

4. Results and Discussion

We have formed PS layers of different thicknesses and porosities on several samples by varying the current density and anodic ECE time, and confirmed that the average current density is much higher in the galvanostatic mode (i.e., the current density or potential difference remains constant) than in the potentiostatic mode (i.e., a constant current density). Therefore, a higher porosity is expected in the galvanostatic mode, which involves a higher charge, for obtaining a comparable PS layer thickness in the galvanostatic mode of formation.

The high current density (270 mA/cm^2) and short anodic ECE time (<35 s) resulted in a high-porosity structure, such as mezo-porous structure. The PS surface images in Fig. 3 show that the formation of PS is isotropic and slightly depends on the Si surface crystallographic orientation. Figure 3(c) shows the top view of the PS layer. The surface geometry is a new surface structure composed of a standard texture formed by KOH etching and a mezo-porous substructure with a pore diameter smaller than 50 nm in Fig. 3(c). The alkaline-textured mc-Si gives a weighted reflectance of about 24.1% before PS formation. After PS formation, the weighted reflectance decreases to about 19% in Fig. 5. We consider that observed the interesting mezo-porous spongelike structure is suitable as an ARC for light

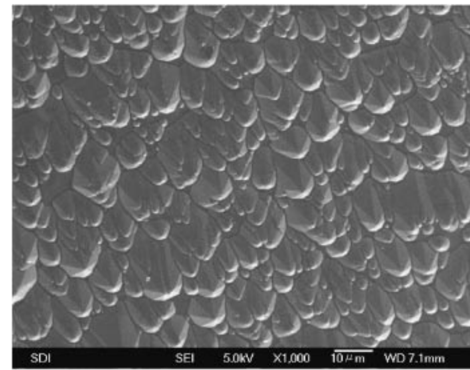

(a)

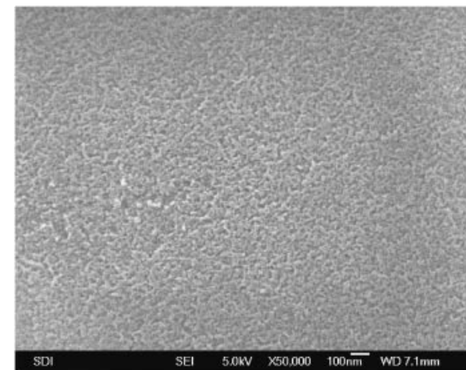

(b)

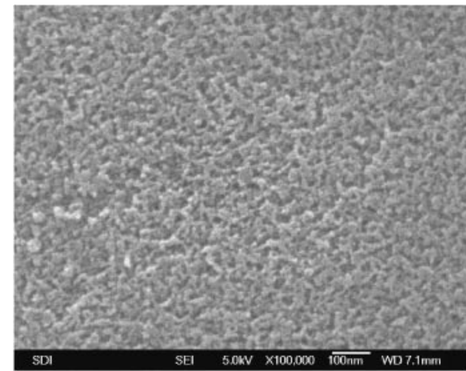

(c)

Fig. 3. FE-SEM image taken from PS sample surface prepared using $Q = 5.2\,C/cm^2$ in HF : EtOH electrolyte with volumetric ratio of 3 : 1. (a) PS formation after alkaline-textured mc-Si (×1,000), (b) images of PS sample surface (×50,000) and (c) mezo-porous structure (×100,000).

trapping and light diffusion since the charge density increases, the porosity increases and the index of refraction decreases. In particular, we previously studied the correlation between the reflectance and the surface roughness.[16] The reduction in reflectance could be explained by the higher roughness of the surface after PS formation.

The optical reflectivity of this structure markedly decreased from 24% to about 4%, as presented in Figs. 4(e) and 5. Analyzed by SE,[17] the thickness and porosity of the PS layer obtained by the anodic ECE of Si were 400–500 Å and 80–90%, respectively. Visually, a top PS layer exhibited still homogeneous blue color and could be sufficiently used as an ARC for solar cells.

Figure 4 shows the weighted reflectance as a function of

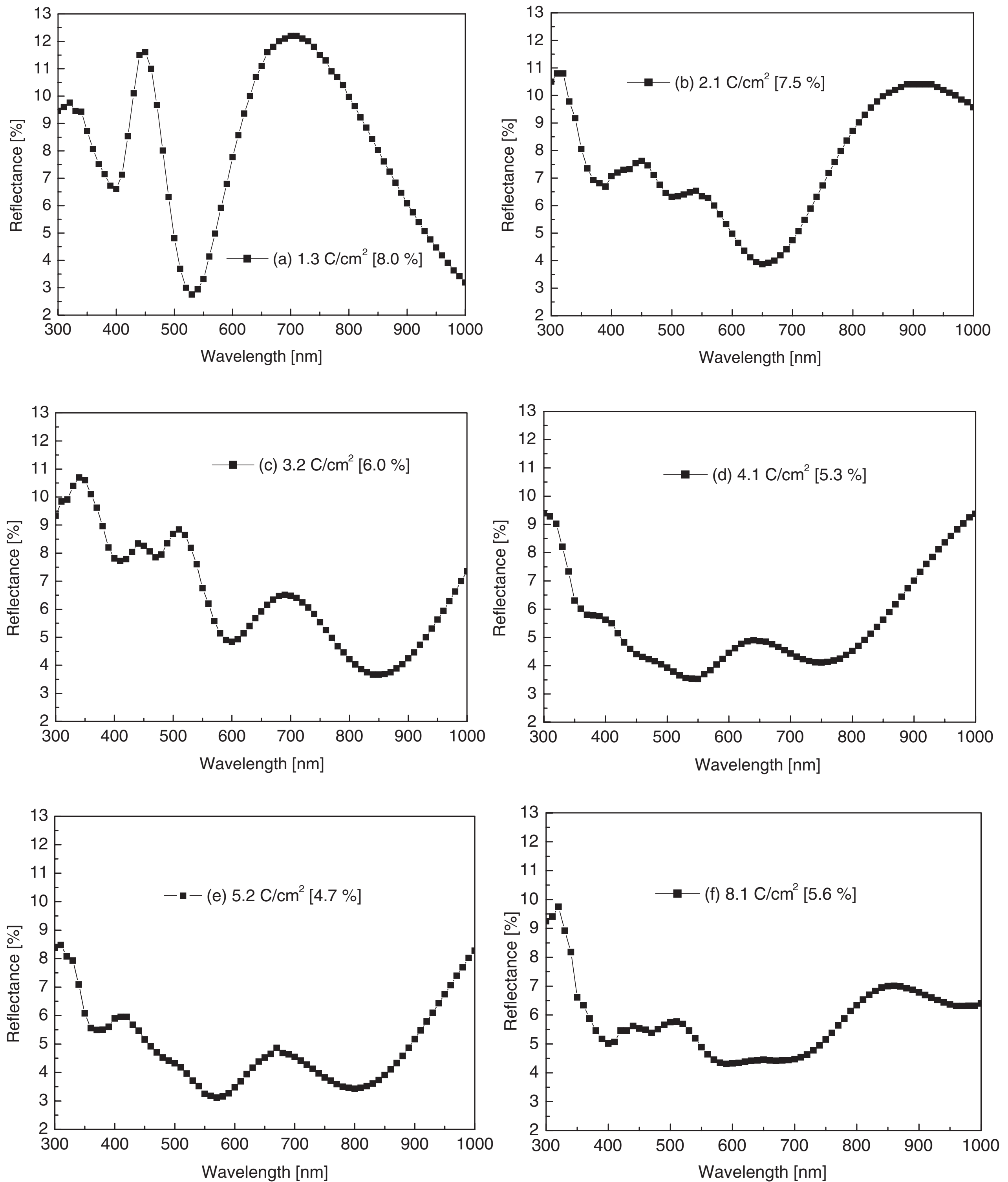

Fig. 4. Plots of measured integral reflectance of PS films grown at 1.3, 2.1, 3.2, 4.1, 5.2, and 8.1 C/cm^2 in wavelength range of 300 to 1000 nm. These films show weighted reflectances of 8.0 (a), 7.5 (b), 6.0 (c), 5.3 (d), 4.7 (e), and 5.6% (f).

wavelength for six samples with $Q = 1.3$, 2.1, 3.2, 4.1, 5.2, and 8.1 C/cm^2. The reflectance decreased to less than 5% for $Q = 5.2\,C/cm^2$, between 400 and 1000 nm. This value was compared with that obtained with the KOH-textured mc-Si surface covered with an optimized SiN_X ARC layer, as shown in Fig. 5. The reflectance spectra in Figs. 4(a)–4(f) provide the optical properties of the PS film. The specific form of the reflectance spectra of the grains covered with a PS layer is due to interference effects in the layer, which implies that the PS layer has different optical properties compared with bulk silicon.[18] Figures 4(a)–4(f) show the relationship between increases in porosity and decreases in reflective index for PS films. The number of modulations in the spectra directly corresponded to the number of various refractive indexes in the PS layer. A further increase in Q did not significantly change the reflectance. When using high charge densities ($>8.1\,C/cm^2$), the modulations may not be observed at all, because the PS layer obtained by anodic

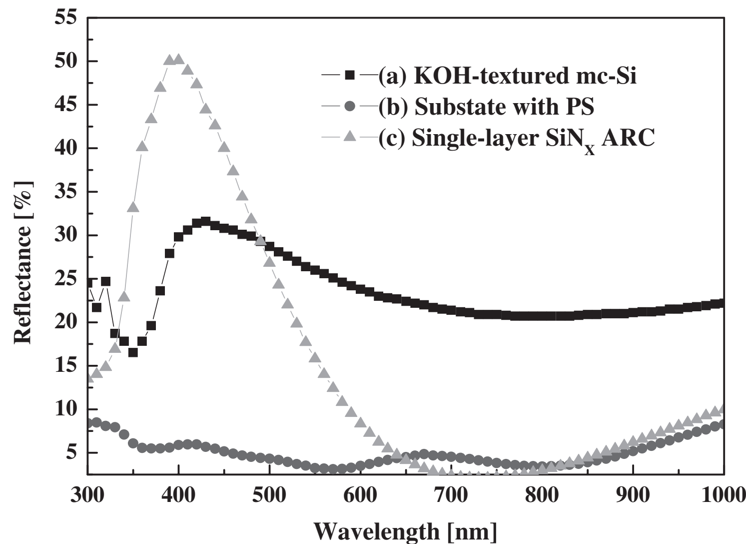

Fig. 5. Reflectance characteristics of (a) alkaline-textured mc-Si wafer, (b) PS antireflective layer, and (c) single-layer SiN_X ARC.

ECE is peeled off. We observed a flaked and deteriorated PS film generated at 9.5 C/cm^2.

The integral reflectance of PS shown in Fig. 4(e) has a much lower weighted reflectance of 4.44% than that of 5.58% shown in Fig. 4(f) in the wavelength range of 650 to 700 nm. The wavelength range is important for photovoltaic applications due to the energy content of the solar spectrum peaks in that range. The decrease in reflectance in the sensitivity range of the solar cell increases the short-circuit current density (I_{sc}). The minimum reflectance occurs at a charge density of 5.2 C/cm^2. In addition, the PS structure is generally assumed to give rise to quantum confinement and an increased band gap. The wide band gap of PS might be useful for establishing a minority carrier mirror, which could contribute to surface passivation.

Figure 5 shows that the additional PS antireflective layer after the alkaline-textured mc-Si wafer results in a decrease in reflectance. It is clearly observed that the reflectance of the PS antireflective layer used in the further experiments has a minimum of 3.1% at 570 nm, while the SiN_X ARC reflectance has a minimum of 2.0% at 730 nm. As a result, the integral reflectance of the PS used as an ARC is about 4% in the wavelength range of 400 to 1000 nm and 8% less than that of a commercial SiN_X ARC. Moreover, we compared the reflectance characteristics of the optimized SiN_X layer coated (thickness of 700–800 Å) by PECVD with a PS layer.

A comparison of the optimal PS antireflective layer formed on the alkaline-textured mc-Si surface and the conventional SiN_X ARC formed on the alkaline-textured mc-Si surface shows some advantages. First, the PS antireflective layer is uniformly formed on the entire area of the mc-Si wafer, which is almost independent of grain orientation, while conventional alkaline texturing only works well in the case of mono-Si. Secondly, the PS antireflective layer demonstrates an optical performance superior to most vacuum-deposited ARC layers. It is expected that the perfect light diffuser for a broad wavelength could be used as an antireflective layer without other ARC materials. Moreover, PS has some passivating capabilities that allow fabricating solar cells without an additional passivation coating.

The method of anodic ECE considerably exceeds the conventional methods of chemical anisotropic and mechanical texturing in the efficiency of optical loss reduction by decreasing the weighted reflectance in the range of the 400 to 1000 nm from 24 to 4%. In addition, the ECE method allows a forming texture on the surface of previously created solar cells both before the deposition of the frontal contact comb and after its formation without an additional photolithography process. Because of this, the technological process of solar cell structure creation is simplified.

5. Conclusions

This study demonstrates that, by PS antireflective layer optimization, it is possible to create a new Si surface structure morphology. This layer acts as a perfect light diffuser and provides an appropriate reflectance that is comparable with the reflectance of an alkaline-textured Si surface covered with a conventional SiN_X ARC layer. The simplicity and low cost of the anodic ECE technique, as well as its adaptation to silicon solar cell manufacturing, provide a very promising technology in an industrial process.

Acknowledgments

We thank Dae-Woon Kim (Samsung SDI Co., Ltd., Corporate R&D Centre, Energy Lab., Suwon, Republic of Korea) for providing for preparation of this work. We are indebted to Dong-Seop Kim (Georgia Institute of Technology, Atlanta, GA 30332, U.S.A.) for discussion.

1) H. Takato, M. Yamanaka, Y. Hayashi, R. Shimokawa, I. Hide, S. Gohda, F. Nagamine and H. Tsuboi: Jpn. J. Appl. Phys. **31** (1992) L1665.
2) H. Saha, S. K. Datta, K. Mukhopadhyay, S. Banerjee and M. K. Mukherjee: IEEE Trans. Electron Devices **39** (1992) 1000.
3) L. Asinovsky, F. Shen and T. Yamaguchi: Thin Solid Films **313–314** (1998) 198.
4) P. Campbell and M. A. Green: J. Appl. Phys. **62** (1987) 243.
5) R. W. Fathauer, T. George, A. Ksendzov and R. P. Vasquez: Appl. Phys. Lett. **60** (1992) 995.

6) S. W. Park, J. Kim and S. H. Lee: J. Korean Phys. Soc. **43** (2003) 423.
7) E. A. Starostina, V. V. Starkov and A. F. Vyatkin: Russ. Microelectron. **31** (2002) 88.
8) A. Prasard, S. Balakrishnan, S. K. Jain and G. C. Jain: J. Electrochem. Soc. **129** (1982) 596.
9) C. Lévy-Clément, A. Lagoubi, M. Neumann-Spallart, M. Rodot and R. Tenne: J. Electrochem. Soc. **138** (1991) L69.
10) J. H. Kwon, D. S. Kim and S. H. Lee: 205th Meet. Electrochem. Soc., May 9–14, San Antonio, Texas, U.S.A., 2004, L1-0398.
11) R. R. Bilyalov, R. Lüdemann, W. Wettling, L. Stalmans, J. Poortmans, J. Nijs, L. Schirone, G. Sotgiu, S. Strehlke and C. Lévy-Clément: Sol. Energy Mater. Sol. Cells **60** (2000) 391.
12) A. Uhlir: Bell Syst. Tech. J. **35** (1956) 333.
13) V. Vehmann and H. Foll: J. Electrochem. Soc. **137** (1990) 653.
14) M. Rauscher and H. Spohn: Phys. Rev. E **64** (2001) 031604.
15) P. Allongue, V. Kieling and H. Gerischer: Electrochim. Acta **40** (1995) 1353.
16) R. J. Martín-Palma, L. Vázquez, J. M. Martínez-Duart, M. Schnell and S. Schaefer: Semicond. Sci. Technol. **16** (2001) 657.
17) M. Fried, O. Polgár, T. Lohner, S. Strehlke and C. Levy-Clement: J. Lumines. **80** (1998) 147.
18) R. Bilyalov, C. S. Solanki, J. Poortmans, O. Richard, H. Bender, M. Kummer and H. von Känel: Thin Solid Films **403–404** (2002) 170.